Normalized photoacoustic techniques for thermal diffusivity measurements of buried layers in multilayered systems

J. A. Balderas-López,[a] A. Mandelis, and J. A. García
Photothermal and Optoelectronic Diagnostics Laboratories (PODL), Department of Mechanical and Industrial Engineering, University of Toronto, 5 King's College Road, Toronto, Ontario M5S 3G8, Canada

(Received 7 February 2002; accepted for publication 25 June 2002)

The one-dimensional heat diffusion problem for a three-layer system is solved assuming the surface absorption model. The analytical solution is shown to be suitable for the implementation of normalized depth-profilometric photoacoustic methodologies involving the open photoacoustic-cell configuration for thermal diffusivity measurements in buried underlayers within a three-layer stack. Our normalization procedures eliminate the frequency-dependent instrumental electronic contribution (transfer function) and some thermophysically nonrelevant proportionality factors in the theoretical equations, thus making the depth-profilometric analysis feasible. The measurement methodology is achieved by normalizing the theoretical photoacoustic signal from the three layers with the corresponding signal from the uppermost two layers, involving linear fits to measure the thermal diffusivity of the third underlayer. Three different multilayered materials were examined using the proposed methodologies. High reproducibility of the thermal diffusivity measurements and good agreement with values reported in literature were found. Besides the foregoing procedures, a lumped photoacoustic model was developed, which yields the effective thermal-diffusivity value of the multilayer stack. © *2002 American Institute of Physics.* [DOI: 10.1063/1.1500784]

I. INTRODUCTION

Photothermal (PT) techniques have become popular measurement methodologies for thermal and optical characterization of solids and liquids.[1–10] Among the various types of PT techniques the photoacoustic (PA) method is widely used for carrying out thermal diffusivity measurements in solids.[4–10] The transmission PA configuration involving the surface absorption model is generally used for this purpose.[5–10] The main assumption in the surface absorption model is that the light is absorbed within an infinitesimal depth compared to the thermal diffusion length inside the sample. The analytical equation for the PA signal resulting from this model contains the optical absorption coefficient of the medium only as a linear proportionality factor, which can be subsequently eliminated by an adequate normalization procedure. This is in contrast to the nonlinear dependence on the optical absorption coefficient of the equations resulting from the use of distributed optical absorption, such as the Beer–Lambert model. Moreover, when the surface absorption model is used, the transmission of the thermal wave across the sample is exponentially damped with the thermal diffusion length in the medium as the characteristic damping distance (skin depth), thus allowing accurate measurements of the thermal diffusivity. Unfortunately, the application of the surface absorption model is strictly limited to metallic and other highly opaque absorbers. Therefore, when the method is applied to the thermophysical characterization of single-layered dielectric materials, it becomes necessary to attach a metal cover layer on top of the sample. The situation becomes more complicated in the case of a bilayer material. Therefore, practical use of PA techniques in the characterization of dielectric material thermophysical properties requires consideration of a multilayer model with an opaque thin-film overlayer. In literature, several generalized theories dealing with thermal-wave diffusion across multilayered materials have been reported,[11–13] however, they have found limited application for practical thermal characterizations due to their apparent complexity: They either assume distributed optical absorption[12,13] or are multidimensional, so that solutions are given in integral mode.[13] With simplification in mind and for purposes of clarity, in this article, the one-dimensional heat diffusion theoretical model for a three-layer solid stack with a harmonic surface heat source is solved. A one-dimensional theoretical expression for the photothermal signal is explicitly derived and it is shown to be useful toward the implementation of signal-normalized methodologies for depth-profilometric thermal diffusivity measurements on single- and two-layer dielectric solids embedded in three-layer stacks. Although data normalization in PT techniques is commonplace, especially for photopyroelectric and radiometric techniques,[14,15] its implementation for open PA cell (OPC) methodologies is relatively new.[10] Data normalization in PA techniques is very useful: Through it, the instrumental electronic frequency response (transfer function) and some other nonessential frequency-independent signal-related proportionality constants (especially when only surface absorption is involved) can be conveniently eliminated. Therefore, the number of required known-parameter inputs is

[a]Also at: Unidad Profesional Interdisciplinaria de Biotecnología del IPN, Avenida Acueducto S/N, Col. Barrio la Laguna, Del. Gustavo A. Madero, C. P. 07340, Mexico, D. F., México;
electronic mail: abrahambalderas@hotmail.com

reduced, making the depth-profilometric analysis feasible, simple, and reliable. Balderas-López and Mandelis[10] have considered the case of bilayer materials (a metal layer on top of a dielectric material) and a very convenient normalization procedure for simplifying the analysis was developed. In this article, the foregoing normalization procedure has been extended to thermal diffusivity measurements in two-layered systems buried in a three-layer stack. As a side benefit, use of the analytical equations from the three-layer model yields a very convenient and practical depth-profilometric normalization methodology involving linear data fits. The latter method is developed for measuring the thermal diffusivity of the bottom layer buried in a three-layer stack. Experimentally, three materials were used as buried underlayers to validate the PA methodologies reported in this work: Polyvinylidene difluoride (PVDF) piezoelectric film, laser printer acetate film, and glass. High reproducibility and good agreement with values reported in literature were demonstrated.

II. THEORETICAL CONSIDERATIONS

A. Mathematical model

The geometry of the general one-dimensional model, depicted in Fig. 1, consists of three layers embedded between two semi-infinite, optically nonabsorbing, media. Assuming that modulated light with intensity I_0 and angular modulation frequency $\omega=2\pi f$ impinges on the upper surface of medium m (Fig. 1), and considering only the surface absorption limit, the corresponding one-dimensional differential equations for the one-dimensional heat diffusion problem, valid in the limit of uniform optical excitation intensity and beam size large compared to the thickness of the multilayer system, are

$$\frac{\partial^2 T_w}{\partial x^2}-\frac{1}{\alpha_w}\frac{\partial T_w}{\partial t}=0 \quad 0\leqslant x$$

$$\frac{\partial^2 T_m}{\partial x^2}-\frac{1}{\alpha_m}\frac{\partial T_m}{\partial t}=-\frac{\beta I_0\delta(x)}{2k_m}[1+e^{i\omega t}] \quad -\ell\leqslant x\leqslant 0$$

$$\frac{\partial^2 T_i}{\partial x^2}-\frac{1}{\alpha_i}\frac{\partial T_i}{\partial t}=0 \quad -\ell-\Delta\leqslant x\leqslant -\ell \tag{1}$$

$$\frac{\partial^2 T_s}{\partial x^2}-\frac{1}{\alpha_s}\frac{\partial T_s}{\partial t}=0 \quad -\ell-\Delta-L<x\leqslant -\ell-\Delta$$

$$\frac{\partial^2 T_g}{\partial x^2}-\frac{1}{\alpha_g}\frac{\partial T_g}{\partial t}=0 \quad -\infty<x\leqslant -\ell-\Delta-L.$$

Here T_j, α_j, $j=w$, m,i,s,g, correspond to the oscillating temperature and thermal diffusivity of medium j, respectively. w and g stand for the semi-infinite ambient layers surrounding the three-layer structure with coordinates $x>0$ and $x<-\ell-L-\Delta$, respectively. β is the absorption coefficient of the absorbing medium m (surface only) and k_m is the corresponding thermal conductivity. Solving this system of coupled equations with the proper boundary conditions of heat flux and temperature continuity at all interfaces, and the physical requirement of finite solutions as $x\to\pm\infty$, the resulting time-harmonic temperature oscillation in medium g is

$$T_g(x,t)=\frac{I_0\beta d}{4k_m\sigma_m}\frac{(1+\gamma_{wm})(1-\gamma_{mi})(1-\gamma_{is})(1-\gamma_{sg})e^{-\sigma_m\ell}e^{-\sigma_i\Delta}e^{-\sigma_s L}e^{\sigma_g(x+\ell+\Delta+L)}e^{i\omega t}}{D_3}, \tag{2}$$

where

$$\begin{aligned}D_3=&1+\gamma_{is}\gamma_{sg}e^{-2\sigma_s L}+\gamma_{mi}\gamma_{is}e^{-2\sigma_i\Delta}\\&+\gamma_{mi}\gamma_{sg}e^{-2\sigma_i\Delta}e^{-2\sigma_s L}+\gamma_{wm}\gamma_{mi}e^{-2\sigma_m\ell}\\&+\gamma_{wm}\gamma_{mi}\gamma_{is}\gamma_{sg}e^{-2\sigma_s L}e^{-2\sigma_m\ell}\\&+\gamma_{wm}\gamma_{is}e^{-2\sigma_i\Delta}e^{-2\sigma_m\ell}\\&+\gamma_{wm}\gamma_{sg}e^{-2\sigma_m\ell}e^{-2\sigma_i\Delta}e^{-2\sigma_s L}.\end{aligned} \tag{3}$$

In this equation, d is the thickness of the infinitesimal layer in material m (see Fig. 1) where the incident light is absorbed entirely; $\sigma_j=(1+i)a_j$, (j as before), where $a_j=(\pi f/\alpha_j)^{1/2}$ is the thermal diffusion coefficient, and γ_{jk} are thermal coupling coefficients (the so-called thermal-wave reflection coefficients) defined as $\gamma_{jk}=(1-e_j/e_k)/(1+e_j/e_k)$, where $e_j=k_j/\alpha_j^{1/2}$, is the thermal effusivity of medium j. In the OPC configuration, g is the transport medium in which the PT effect is detected in transmission (the air inside the PA chamber). Using the Rosencwaig–Gersho model,[16] it is easy to show that the pressure (PA) signal corresponding to the harmonic temperature oscillation of Eq. (2) is given by

$$\delta P_3(f,t)=\frac{\gamma P_0 I_0 G(f)\beta d}{4\sqrt{2}T_0\ell_g k_m a_g\sigma_m}\frac{(1+\gamma_{wm})(1-\gamma_{mi})(1-\gamma_{is})(1-\gamma_{sg})e^{-\sigma_m\ell}e^{-\sigma_i\Delta}e^{-\sigma_s L}e^{i\omega t}}{D_3}, \tag{4}$$

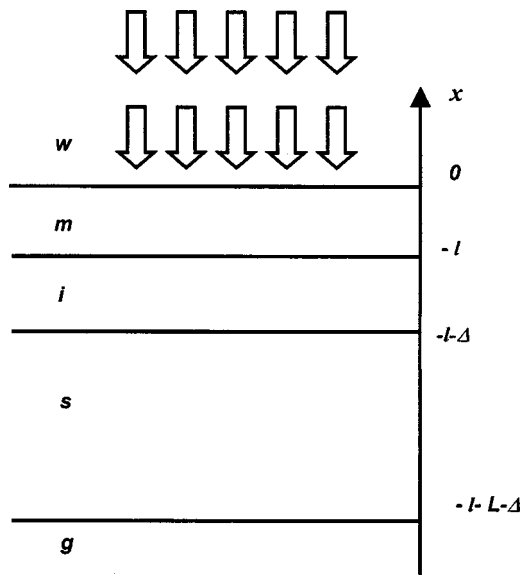

FIG. 1. Schematic representation of the one-dimensional multilayer photoacoustic model with surface absorption. *w*: glass substrate; *m*: metal layer with surface absorption coefficient β at $x=0$; *i*: interlayer material; *s*: sample; and *g*: gas.

where P_0 and T_0 are the ambient pressure and temperature, respectively, for the air inside the PA chamber, γ is the specific heat ratio for air, $\gamma=c_p/c_v$, and ℓ_g is the thickness of the air layer. The experimental PA signal is multiplied by a modulation-frequency-dependent factor, $G(f)$, representing the influence of the instrumental transfer function.

B. Special limiting cases

1. Single layer

On the assumption that in Eq. (4) media, i, s and g are the same material, the three-layer system shown in Fig. 1 transforms effectively into a one-layer system involving only a single material (m) of thickness ℓ. The corresponding PT expression for a surface-absorbing medium surrounded by two semi-infinite media is obtained as a limiting case. Under this assumption $\gamma_{sg}=\gamma_{is}=0$, and Eq. (4) simplifies to

$$\delta P_1(f,t)=\frac{\gamma P_0 I_0 \beta d(1+\gamma_{wm})(1-\gamma_{mg})e^{i\omega t}}{4\sqrt{2}T_0\ell_g k_m\sigma_m a_g}\times\frac{e^{-\sigma_m\ell}}{[1+\gamma_{wm}\gamma_{mg}e^{-2\sigma_m\ell}]} \tag{5}$$

The thermally thick limit of this equation has been used extensively for thermal diffusivity measurements of solids.[1,5,7] For non-opaque materials, attaching a thin metal foil on top of the solid under evaluation has become a popular practice.[5–7] Furthermore, the single-layer model has been used to obtain the effective thermal diffusivity of two-layered materials in series by making use of electrical and thermal analogies and taking the thermoelastic limit for the PA signal from this single layer model.[7]

2. Two layers

In a similar manner, if media s and g are considered to be identical, the three-layer system of Fig. 1 readily transforms into a two-layer system involving only materials m and i. In this limit, $\gamma_{sg}=0$ and Eq. (4) simplifies to the corresponding equation for the PA signal from two layers reported by Balderas–López and Mandelis[10]

$$\delta P_2(f,t)=\frac{\gamma P_0 I_0 G(f)\beta d}{4\sqrt{2}T_0\ell_g k_m a_g\sigma_m}\frac{(1+\gamma_{wm})(1-\gamma_{mi})(1-\gamma_{ig})e^{-\sigma_m\ell}e^{-\sigma_i\Delta}e^{i\omega t}}{(1+\gamma_{mi}\gamma_{ig}e^{-2\sigma_i\Delta}+\gamma_{wm}\gamma_{mi}e^{-2\sigma_m\ell}+\gamma_{wm}\gamma_{ig}e^{-2\sigma_m\ell}e^{-2\sigma_i\Delta})} \tag{6}$$

In Eq. (6), if medium w is assumed to be the same as medium g, a spatial symmetry for the two-layered system follows. This symmetry implies that, aside from the corresponding optical properties (the product βd), the same PA signal will be expected, regardless of which surface is exposed to the modulated light. Mathematically, this fact is expressed by the following property

$$\frac{\delta P_{mi}(f)}{\beta_m d_m}=\frac{\delta P_{im}(f)}{\beta_i d_i}, \tag{7}$$

where $\delta P_{im}(f)$ refers to the PA signal when the interface (*im*) is exposed to the modulated radiation, and vise versa for $\delta P_{mi}(f)$. It is easy to derive Eq. (7) by making use of the antisymmetry property $\gamma_{ij}=-\gamma_{ji}$ between the thermal coupling coefficients and of the fact that $(1-\gamma_{ij})/(1+\gamma_{ij})=e_i/e_j$. It is important to emphasize this spatial symmetry because it contradicts a claim[9] according to which, performing PA experiments with intensity-modulated light impinging on opposite surfaces of a two-layer material, different thermal diffusivity values should be expected for optically opaque solid bilayers. Based on the symmetry indicated by Eq. (7) any directional dependence of the effective thermal diffusivity of a solid layer stack is clearly impossible. This spatial symmetry also follows for the three-layer system.

C. Effective thermal diffusivity for a multi-layer system

Using PT techniques in the transmission configuration, it can be shown that lumped (effective) thermal diffusivity in-

formation about a multilayer system may only be defined in the thermally thick frequency regime. In this limiting case, the term D_3 in the denominator of Eq. (4) and the respective terms in Eqs. (5) and (6) all become unity. The thermal wave is exponentially damped across the thickness of each layer of the sample. It is thus possible to define the effective thermal diffusivity α_{eff} for two- or three-layered systems, by making the thermal analogy with the single-layer system, and using the following relations (corresponding to thermal diffusion transit times across the relevant layers):

$$\frac{L_2}{\sqrt{\alpha_{\text{eff}}}}=\frac{\ell}{\sqrt{\alpha_m}}+\frac{\Delta}{\sqrt{\alpha_i}}, \tag{8a}$$

$$\frac{L_3}{\sqrt{\alpha_{\text{eff}}}}=\frac{\ell}{\sqrt{\alpha_m}}+\frac{\Delta}{\sqrt{\alpha_i}}+\frac{L}{\sqrt{\alpha_s}}, \tag{8b}$$

where $L_2=\ell+\Delta$ and $L_3=\ell+\Delta+L$. The same conclusion was reached by Salazar *et al.*[17] and John *et al.*[18] The latter investigators obtained the symmetry property by use of a transmission mode photopyroelectric configuration of multilayers. Moreover, following the same assumptions, it is easy to infer the generalized equation for the effective thermal diffusivity of an *n*-layer system:

$$\frac{L_n}{\sqrt{\alpha_{\text{eff}}}}=\Sigma_{j=1}^{n}\frac{\ell_j}{\sqrt{\alpha_j}} \tag{9}$$

where $L_n=\Sigma_{j=1}^{n}\ell_j$. It is important to emphasize again that this PT analogy is well-defined only for thermally thick multilayers. Trying to extend this analogy to other thermal regimes leads to modulation-frequency-dependent effective thermal diffusivities.[8] This notion is physically unacceptable, as thermal diffusivity is an intrinsic property of a given material and, in the case of thermally homogeneous solids, it can not change with the modulation frequency of the excitation light source. This definitional inadequacy can be easily corrected by considering the thermal-wave impedance of a composite solid, a quantity which is frequency dependent (Ref. 19).

D. Normalized photoacoustic techniques

It is possible to determine the thermal diffusivity of solids by use of Eqs. (4)–(6). In particular, by normalizing the PA signal for the three-layer material with the corresponding signal from the first (uppermost) layer alone, it is possible to develop a PA methodology for extracting the effective thermal diffusivity in two-layered materials. The normalization procedure developed by Balderas–López and Mandelis[10] can then be applied. Moreover, by normalizing the PA signal from three layers with the corresponding signal from the two uppermost layers, a new PT methodology involving simple linear fits to measure the thermal diffusivity of the third (buried) underlayer is possible.

1. Depth-profilometric measurement of the thermal diffusivity of a buried underlayer by use of the three-layer model

On taking the ratio of Eqs. (4) and (6), it is possible to develop a normalization procedure for the thermal diffusivity measurement of layer s in Fig. 1. Through this, procedure, all common proportionality factors and the instrumental transfer function, $G(f)$, are eliminated and the following simple relation is obtained

$$\frac{\delta P_3}{\delta P_2}=\left(\frac{D_2}{D_3}\right)\frac{(1-\gamma_{is})(1-\gamma_{sg})}{(1-\gamma_{ig})}e^{-\sigma_s L} \tag{10}$$

where

$$D_2=1+\gamma_{mi}\gamma_{ig}e^{-2\sigma_i\Delta}+\gamma_{wm}\gamma_{mi}e^{-2\sigma_m\ell}+\gamma_{wm}\gamma_{ig}e^{-2\sigma_m\ell}e^{-2\sigma_i\Delta}.$$

For thermal diffusivity measurements of the layer s, the modulation frequency can be adjusted so that this layer becomes thermally thick. Under this condition, the ratio D_2/D_3 simplifies to

$$\frac{D_2}{D_3}=\frac{1+\gamma_{mi}\gamma_{ig}e^{-2\sigma_i\Delta}+\gamma_{wm}\gamma_{mi}e^{-2\sigma_m\ell}+\gamma_{ig}\gamma_{wm}e^{-2\sigma_m\ell}e^{-2\sigma_i\Delta}}{1+\gamma_{mi}\gamma_{is}e^{-2\sigma_i\Delta}+\gamma_{wm}\gamma_{mi}e^{-2\sigma_m\ell}+\gamma_{is}\gamma_{wm}e^{-2\sigma_m\ell}e^{-2\sigma_i\Delta}} \tag{11}$$

Equations (10) and (11) are still too complicated to give a practical PA measurement technique of the thermal diffusivity of material s. However, a substantial simplification is obtained if the frequency is high enough so that the overlayer i is also thermally thick. If this condition applies, then $\exp(-2\sigma_i\Delta)\cong 0$ and the ratio D_2/D_3 becomes unity, regardless of the thermal behavior of overlayer m. So in the thermally thick regime for sample s and interlayer i, the PA signal takes on the simpler form

$$\frac{\delta P_3}{\delta P_2}=\frac{(1-\gamma_{is})(1-\gamma_{sg})}{(1-\gamma_{ig})}e^{-\sigma_s L}. \tag{12}$$

It is now possible to carry out PA measurements of the thermal diffusivity of layer (s) by making linear fits of the ratio of experimental data expressed by Eq. (12), on a semilog scale. From the experimental point of view, the use of an interlayer (material i) with a known low thermal diffusivity value is required to ensure the thermally thick behavior of the layer starting from very low modulation frequencies. In this manner, any change of the normalized photothermal signal can be associated with the photothermal behavior of the layer (s), the thermal diffusivity of which is to be measured. Obtaining a linear behavior on the semilog scale is, indeed, the desired confirmation that the experimental conditions match the theoretical assumptions.

2. Measurement of the effective thermal diffusivity of bilayers

On taking the ratio of Eqs. (4) and (5), it is clear that the transfer function $G(f)$ and all common proportionality factors are eliminated and the following relation is obtained

$$\frac{\delta P_3}{\delta P_1}=\left(\frac{D_1}{D_3}\right)\frac{(1-\gamma_{mi})(1-\gamma_{is})(1-\gamma_{sg})}{(1-\gamma_{mg})}e^{-\sigma_i\Delta}e^{-\sigma_s L}, \tag{13}$$

where

$$D_1=1+\gamma_{wm}\gamma_{mg}e^{-2\sigma_m\ell}$$

As was just shown for the purpose of defining an effective thermal diffusivity, it is required that each of the layers i and s of the multilayer should be thermally thick. Under this assumption, $\exp(-2\sigma_i\Delta)\cong 0\cong\exp(-2\sigma_s L)$ and the ratio D_1/D_3 simplifies to

$$\frac{D_1}{D_3}=\frac{1+\gamma_{wm}\gamma_{mg}e^{-2\sigma_m\ell}}{1+\gamma_{wm}\gamma_{mi}e^{-2\sigma_m\ell}}. \tag{14}$$

Adjusting the modulation frequency so that the overlayer m is thermally thin, one may set $\exp(\pm\sigma_m\ell)\cong 1\pm\sigma_m\ell$. Therefore, it is possible to rewrite Eq. (13) in the simpler form

$$\frac{\delta P_3}{\delta P_1}=\frac{(1-\gamma_{mi})(1-\gamma_{is})(1-\gamma_{sg})}{(1-\gamma_{mg})}\frac{(1+\gamma_{wm}\gamma_{mg})}{(1+\gamma_{wm}\gamma_{mi})}\times\left[\frac{1+\dfrac{(1-\gamma_{wm}\gamma_{mg})}{(1+\gamma_{wm}\gamma_{mg})}\sigma_m\ell}{1+\dfrac{(1-\gamma_{wm}\gamma_{mi})}{(1+\gamma_{wm}\gamma_{mi})}\sigma_m\ell}\right]e^{-\sigma_{\rm eff}L_{\rm eff}}, \tag{15}$$

where $L_{\rm eff}=L+\Delta$ and $\sigma_{\rm eff}=(1+i)(\pi f/\alpha_{\rm eff})^{1/2}$. $\alpha_{\rm eff}$ is defined by Eq. (8a) (with $L_{\rm eff}$ instead of L_2, L instead of ℓ, and α_s instead of α_m). It is clear that, but for a constant factor, Eq. (15) is the same as Eq. (13) in Ref. 10. Consequently, the PT technique of Ref. 10 can also be applied to this situation for measurements of the effective thermal diffusivity of a bilayer. Closer examination of Eq. (14) shows that it is theoretically possible to obtain a further simplification of the ratio D_1/D_3 when the material m is thermally thick, however, the experimental procedure faces practical limitations because such an arrangement would require thick and opaque overlayers and/or frequencies that are too high to yield reasonable signal-to-noise ratios. Complicating the issue, thermoelastic and thermal-wave signals are strongly coupled at high modulation frequencies in PA detection and decoupling them is not an easy task. In experimental practice, the normalized data themselves will indicate if this decoupling is possible through the presence of an inflection point on the corresponding plot indicating the start of domination of the thermoelastic behavior. The corresponding modulation frequency can then be used as a natural upper limit to the simple quantitative analysis through Eq. (15).

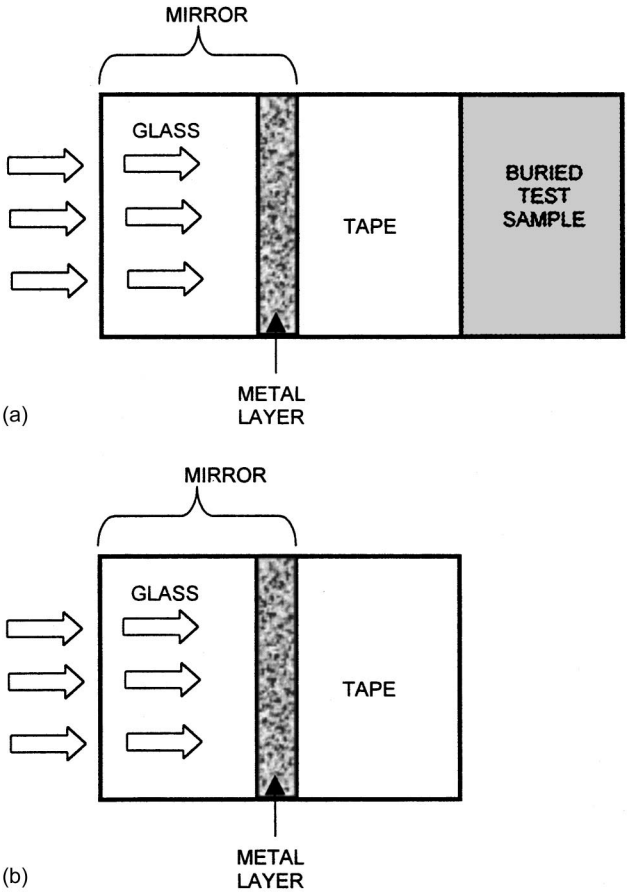

FIG. 2. Cross section of multilayer stack with a double-sided adhesive interlayer. (a) Three-layer stack and (b) Two-layer stack.

III. EXPERIMENTAL

A. Sample preparation

Several three-layer stacks [cross sections are shown in Fig. 2 (a)] were fabricated to demonstrate the applicability of the methodologies described in Secs. II D 1 and II D 2. They consisted of the premetallized surface of a glass mirror as a light-to-heat converter (uppermost layer), double-sided adhesive polymer tape (Manco, Inc.) (second layer) and one of the following test materials (third layer): PVDF polymer film (Piezofilm), laser printer film (Xerox), and a microscope glass slide (Corning). Equation (12) was used for the thermophysical characterization of the materials used as the third underlayer and Eq. (15) was used for that of the bilayer stacks formed by the polymer tape and the various materials used as the third underlayer. To test the reproducibility of the results, three samples of each three-layer stack were prepared by tightly attaching the metallized surface of the mirror (square-shaped pieces of ≈ 1 cm^2 area) and each of the test materials [Fig. 2 (a)] to the opposite surfaces of two-sided adhesive polymer tape. For thermal characterization of the tape [used for verification of Eq. (8a)], and for the purpose of obtaining the reference signal according to the methodology described in Sec. II D 1, three samples of bilayer stacks were prepared by joining one side of the double-sided adhesive tape to the metallized surface of the mirror [Fig. 2 (b)]. The

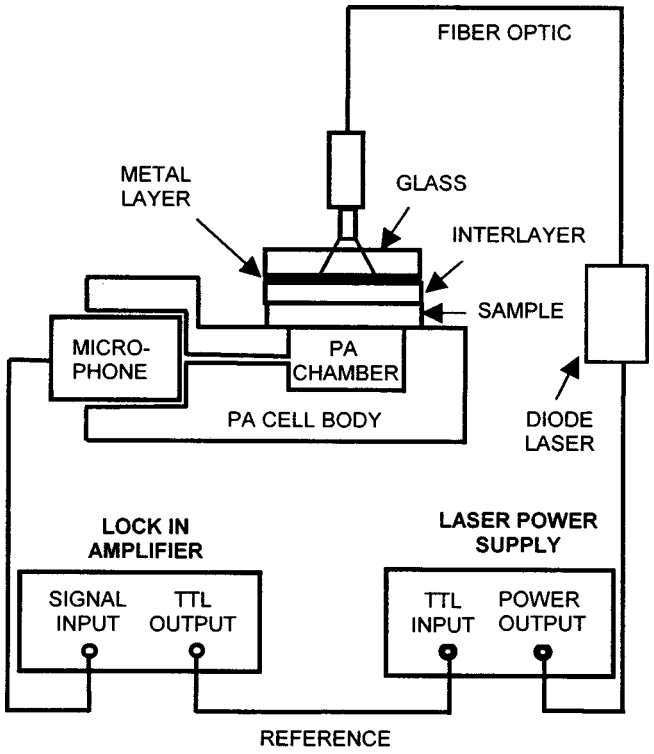

FIG. 3. Schematic cross section of the PA cell transmission configuration experimental setup used for depth-profilometric thermal diffusivity measurements.

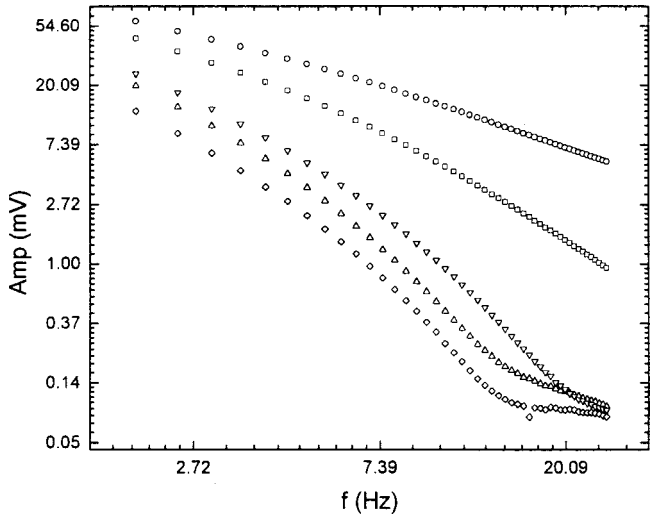

FIG. 4. Typical PA signal amplitudes for the materials and multilayers used in this work. Circles correspond to the PA signal from the bare metal layer; squares correspond to the signal from the metal layer and the interlayer material (adhesive tape); Upside-down triangles correspond to the signal for the three-layered system formed by the metal layer, the tape, and the PVDF film; upright triangles correspond to the signal for the three-layered system formed by the metal layer, the tape and the laser polymer film; diamonds correspond to the signal for the three-layered system formed by the metal layer, the tape, and the glass sample.

glue layer attached to the free surface of the tape was carefully removed by using cotton sticks dipped in acetone.

B. Experimental setup

The experimental PA setup is shown in Fig. 3. It consisted of an infrared (830 nm) semiconductor diode laser with a fiber-optic pigtail (Opto Power Corporation), delivering 60 mW of continuous wave power. Intensity modulation of the laser light was achieved through current modulation of the diode and the modulated radiation entered the nonmetallized surface of the mirror slab (2 mm thick), impinged, and was absorbed on, the metallized surface, (Fig. 2). Thermal waves generated in this metal layer traveled across the multilayer material sample, reaching the PA chamber. The latter consisted of a cylindrical cavity (3 mm diameter and 3 mm height), made of a brass body, communicating with an electret microphone and its built-in preamplifier through a hollow channel (Fig. 3). The PA signal was monitored as a function of the modulation frequency (a frequency scan). The output signal was fed to a lock-in amplifier (LIA) (Stanford Research model SR830) for further amplification and demodulation. The laser current was modulated using the internal oscillator of the LIA to drive the laser power supply via a TTL communications port. One frequency scan was made for the bare metal surface of the mirror (one layer) as a reference signal for thermal diffusivity measurements of the tape and the various two-layer stacks formed from the tape. Another scan was made for each of the test materials, as described in Sec. II D 2 and in Ref. 10. The PA frequency scan for the bilayer stack consisting of the metal layer and the tape, was taken as the reference signal for depth-profilometric thermal diffusivity measurements of the third underlayer of the three-layer stacks by means of the methodology described in Sec. II D 1. Measurement variance statistics were obtained by taking the averages of the measured thermal diffusivity (and effective thermal diffusivities) from three independent measurements of each sample through computing the corresponding standard deviation.

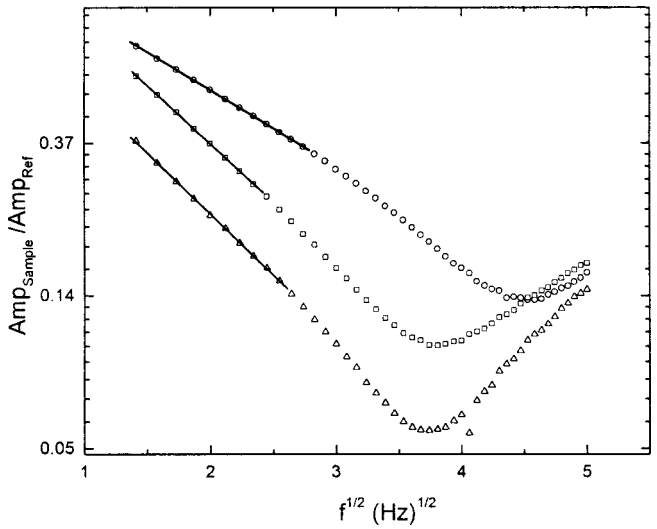

FIG. 5. Normalized PA signal amplitude ratios for the materials measured using the methodology (described in Sec. II D 1). Circles correspond to the normalized signal from the PVDF polymer film; squares correspond to the signal from the laser polymer; upright triangles correspond to the signal for the glass sample; and continuous lines correspond to the best fits to Eq. (12).

TABLE I. Thermal diffusivities, α_{RN}, for the test materials studied in this work, measured by using the normalized PA depth-profilometry reported in Sec. II D 1. One thermal diffusivity value reported in literature for similar materials is also presented (α_{Ref}) for comparison.

Material	Thickness (cm)($\times 10^{-2}$)	α_{RN} (cm^2/s)($\times 10^{-2}$)	α_{Ref} (cm^2/s)($\times 10^{-2}$)
Laser polymer	$L=1.10\pm0.05$	0.055 ± 0.003	···
PVDF polymer	$L=0.60\pm0.05$	0.046 ± 0.005	0.054 (Ref. 20)
Corning glass	$L=1.60\pm0.05$	0.127 ± 0.004	···

TABLE II. Effective thermal diffusivities, α_{eff}, for the bilayer materials studied in this work, measured by using the normalized PA depth-profilometry reported in Sec. II D 2.

Bilayer system	Effective thickness (cm)($\times 10^{-2}$)	α_{eff} (cm^2/s)($\times 10^{-2}$)
Tape and laser polymer	$L=1.70\pm0.10$	0.043 ± 0.003
Tape and PVDF polymer	$L=1.20\pm0.10$	0.038 ± 0.002
Tape and corning glass	$L=2.20\pm0.10$	0.100 ± 0.003

IV. RESULTS AND DISCUSSION

Figure 4 shows typical PA signal amplitudes as functions of the modulation frequency for all materials and multilayers involved in this work. Figure 5 shows the normalized PA amplitude signal ratio from the bilayer formed by the metal layer and the adhesive tape taken as a reference, and the three-layered stacks under study. The goal was to measure the thermal diffusivity of the third underlayer, by following the methodology described in Sec. II D 1. It is evident that there is a frequency range where there exists a linear region of the amplitude ratio as a function of the square root of the modulation frequency, as predicted by Eq. (12). This is an experimental confirmation that in this range, both materials (the interlayer and the sample) are thermally thick. The continuous straight lines in Fig. 5 are the best fits to this equation. The cutoff frequency for the analysis by means of Eq. (12) was taken as the frequency of the departure from linear behavior in the corresponding plots. The resulting thermal diffusivity values for all test samples are summarized in Table I, column 3. To test self-consistency between the two methodologies described in Secs. D II 1 and D II 2 and verify Eq. (8a), the thermal diffusivity for the plastic polymer tape was measured. For this purpose, the signal from the bilayer formed by the metallic layer and the polymer tape [Fig. 2(b)] was normalized with the corresponding signal from the metallic layer alone and the normalized data were analyzed by the methodology described in Ref. 10. The resulting normalized PA amplitude is shown in Fig. 6 (circles). The continuous line corresponds to the best fit to Eq. (13) in Ref. 10, which is equivalent to Eq. (15) in the present context. The thermal diffusivity for this tape was measured to be $(36\pm3)\times10^{-5}$ cm^2/s. In the same figure, the corresponding normalized signals from the two layers formed by the tape and the materials under examination (PVDF, laser printer polymer, and glass) are shown. These curves were obtained using the corresponding amplitude from the single-metal layer as normalization signal. The continuous lines correspond to the best fits to Eq. (15). Table II, column 3, summarizes the effective thermal diffusivities measured in each case. To verify the validity of Eq. (8a), the thermal diffusivity for the third underlayer [test sample in Fig. 2(a)] was also calculated by means of that equation, using the measured thermal diffusivity values for the various bilayered materials (Table II, column 1) and the thermal diffusivity measured for the plastic adhesive tape. The corresponding results are summarized in Table III, column 3. Comparison among the measured and calculated thermal diffusivity values, columns 2 and 3 in Table III, indicates good agreement, thus demonstrating the utility of the lumped (effective) thermal diffusivity approach for depth-profilometric thermophysical investigations.

Figures 5 and 6 exhibit the well-known exponential damping of the PA signal amplitude in transmission as a function of modulation frequency. As the thermal-wave-generated transmission PA signal becomes weaker with increasing frequency, complicating thermoelastic signal contributions may appear.[10] These contributions are responsible for the nonmonotonic behavior of the various amplitudes and amplitude ratios at high frequencies in Figs. 4–6. These effects suggest the use of modulation frequencies as low as possible, so that the sample will be entirely thermally thick, below the thermoelastic range and, at the same time, there will be adequate signal strength to provide a satisfactory signal-to-noise ratio for the measurement. These results further suggest that the use of an interlayer buffer material with a low thermal diffusivity and thickness, such as the present adhesive tape, ensures thermal thickness at low modulation frequencies and a minimum of thermoelastic contributions.[10] As is experimentally evident from the plots shown in Figs. 4–6, this limit was indeed obtained for the materials used in this work. The use of the double-sided adhesive tape offers evident advantages in terms of mechanical integrity and ease of sample fabrication with good reproducibility, especially

TABLE III. Thermal diffusivities, α, for the test materials studied in this work, measured by using the normalized PA depth-profilometry reported in Sec. II D 1. The corresponding values α_{calc} obtained by means of Eq. (8) with the effective thermal diffusivity value reported in Table. II, column 3, and the thermal diffusivity value measured for the plastic tape, are also shown.

Material	α (cm^2/s)($\times 10^{-2}$)	α_{calc} (cm^2/s)($\times 10^{-2}$)
Laser polymer	0.055 ± 0.003	0.048 ± 0.005
PVDF polymer	0.046 ± 0.005	0.040 ± 0.003
Corning glass	0.127 ± 0.004	0.180 ± 0.004

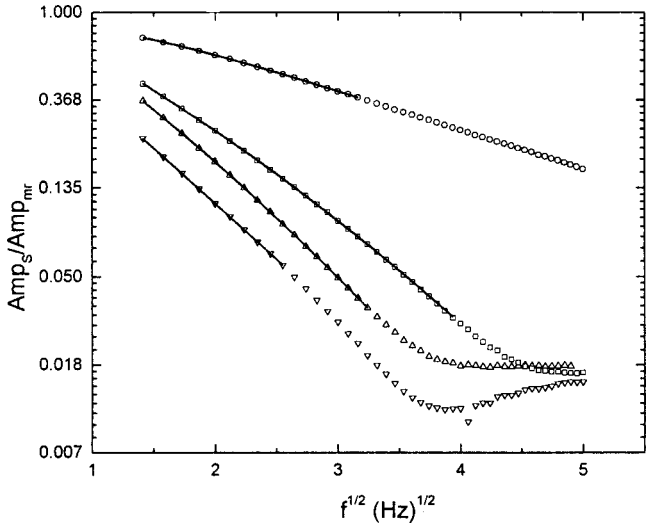

FIG. 6. Normalized PA signal amplitude ratios for the materials measured (using the methodology described in Sec. II D 2). Circles correspond to the normalized signal from the polymer tape; squares correspond to the normalized signal for the bilayer system formed by the tape and the PVDF polymer foil; upright triangles correspond to the signal from the bilayer system formed by the tape and the laser polymer; upside-down triangles correspond to the signal from the bilayer system formed by the tape and the glass sample; and continuous lines correspond to the best fits to Eq. (15).

those used as references for PA amplitude normalization. These procedures, however, may render the introduction of interfacial thermal impedances inevitable. As is evident from the experimental results reported in this work, fortunately, interfacial thermal impedances were not significant here. A self-curable resin (e.g., Torcill™) might be a better choice as interlayer material, if maintaining the constancy of the interlayer buffer thickness becomes a problem. In principle, the same methodologies are equally valid for thermal diffusivity measurements by using the PA phase (in this case, the phase difference between the three-layered sample stacks and the corresponding reference), however, experimentally it was not possible to decouple the thermal PA contribution from the thermoelastic PA contribution for phase signals, unlike the PA amplitude. This is usual for PA methodologies, because the effects of thermoelastic contributions are stronger and cover a wider frequency range in the phase channel than in the amplitude.[21] Efficient normalization procedures like the ones presented here and in Ref. 10, however, represent a powerful tool for identifying the extent of thermoelastic contributions to both channels of the frequency-domain PA signal, whenever this situation arises.[10] This is an important difference and an advantage of normalized PA methodologies, as compared to the nonnormalized methodologies sometimes encountered in literature,[5,8] in which thermoelastic signal dominance is accounted for through the criterion of departure of the modulation-frequency dependence of the amplitude alone from the f^{-1} law predicted by the one-dimensional theory. Our investigations show that, without correcting for the transfer function frequency dependence in *both* amplitude and phase channels, the boundaries of the onset of the thermoelastic regime are more gradual and may lead to inaccurate measurements.

V. CONCLUSIONS

In conclusion, two effective depth-profilometric normalization PA transmission methodologies have been developed for measuring the thermal diffusivity of bilayers and deeply positioned (buried) underlayers in a three-layer stack. The normalized Eqs. (12) and (15) were derived to quantify the PA signals, respectively. The analytical procedure for thermal characterization of single-layer materials involves only simple linear fittings. These methodologies eliminate the requirement for instrumental transfer function considerations and amount to major accuracy and simplicity advantages of the present depth-profilometric analysis over other analytical normalized and nonnormalized measurement techniques based on the same configuration.[5,8,10] In principle, the present techniques are applicable to all solid materials, provided that the experimental configuration fulfills the requirements of the theory, i.e., an opaque and thermally thin (metal) overlayer for thermal diffusivity measurements in two-layer materials, and thermally thick underlayers with no thermoelastic overlaps. In addition, a homogeneous interlayer thermal-coupling thin-film material with uniform thickness and low thermal diffusivity, such as an adhesive tape, is required. The simplicity in sample preparation and analysis make the present technique promising for accurate and reproducible depth-profilometric measurements of the thermal diffusivity of buried material layers which are very difficult or impossible to measure otherwise. These include materials such as paper, glasses, and polymers.

ACKNOWLEDGMENTS

The authors wish to acknowledge the support of the Natural Sciences and Engineering Research Council of Canada (NSERC) through a Research Grant to one of the authors (A.M.).

[1] *Progress in Photothermal and Photoacoustic Science and Technology*, edited by A. Mandelis (Elsevier, New York, 1992), Vol. 1.
[2] A. C. Tam, Rev. Mod. Phys. **58**, 381 (1986).
[3] J. A. Balderas-López, A. Mandelis, and J. A. García, Rev. Sci. Instrum. **71**, 2933 (2000).
[4] C. A. Pelá, S. Rocha, E. de Paula, and O. Baffa, Rev. Sci. Instrum. **69**, 3392 (1998).
[5] C. A. S. Lima, M. B. S. Lima, L. C. M. Miranda, J. Baeza, J. Freer, N. Reyes, J. Ruiz, and M. D. Silva, Meas. Sci. Technol. **11**, 504 (2000).
[6] L. F. Perondi and L. C. M. Miranda, J. Appl. Phys. **62**, 2955 (1987).
[7] A. M. Mansanares, H. Vargas, F. Galembeck, L. Buijs, and D. Bicanic, J. Appl. Phys. **70**, 7046 (1991).
[8] E. Marín, J. L. Pichardo, A. Cruz-Orea, P. Diaz, G. Torres-Delgado, I. Delgadillo, J. J. Alvarado-Gil, J. G. Mendoza-Alvarez, and H. Vargas, J. Phys. D **29**, 981 (1996).
[9] N. Muñoz Aguirre, G. González de la Cruz, Y. G. Gurevich, G. N. Logvinov, and M. N. Kasyanchuk, Phys. Status Solidi B **220**, 781 (2000).
[10] J. A. Balderas-López and A. Mandelis, J. Appl. Phys. **90**, 2273 (2001).
[11] C. Glorieux, J. Fivez, and J. Thoen, J. Appl. Phys. **73**, 684 (1993).
[12] J. Vanniasinkam, A. Mandelis, and S. Buddhudu, J. Appl. Phys. **75**, 8090 (1994).
[13] A. Mandelis, *Diffusion-wave Fields: Mathematical Methods and Green Functions* (Springer, New York, 2001).
[14] J. Caerels, C. Gloreux, and J. Thoen, Rev. Sci. Instrum. **69**, 2452 (1998).
[15] M. E. Rodríguez, A. Mandelis, G. Pan, and J. A. García, J. Appl. Phys. **87**, 8113 (2000).

[16] A. Rosencwaig and A. Gersho, J. Appl. Phys. **47**, 64 (1976).
[17] A. Salazar, A. Sánchez-Lavega, and J. M. Terrón, J. Appl. Phys. **84**, 3031 (1998).
[18] P. K. John, L. C. M. Miranda, and A. C. Rastogi, Phys. Rev. B **34**, 4342 (1986).
[19] A. Mandelis, *Diffusion-wave Fields: Mathematical Methods and Green Functions* (Springer, New York, 2001), Chap. 2.10.
[20] *Technical Manual Kynar Piezo Films* (Pennwalt Corp., Valley Forge, PA, 1987).
[21] F. A. MacDonald and G. C. Wetsel, Jr., J. Appl. Phys. **49**, 2313 (1978).